A Novel Method for Rapid Measurement of Membrane Resistance, Capacitance, and Access Resistance

D. F. Donnelly
Department of Pediatrics, Section of Respiratory Medicine, Yale University School of Medicine, New Haven, Connecticut 06510 USA

ABSTRACT During patch clamp recordings, measurement of passive parameters such as access resistance (R_a), membrane resistance (R_m), and membrane capacitance (C_m) often provides useful information regarding physiological changes in the cell. In particular, an increase in capacitance may indicate vesicle fusion events as occurs during exocytosis. Rapid capacitance changes are usually measured with a phase-sensitive detector set to a phase angle that is independent of resistance changes. However, this angle changes over time and may be difficult to determine in cells with a low membrane resistance. The present paper describes a technique for rapidly measuring R_a, R_m, and C_m by simultaneously applying two harmonic frequencies and calculating the passive parameters from the resultant electrode current. Calibration and operation are independent of the compensation circuit settings that may be set to null most of the electrode current. The technique may be implemented on a standard patch clamp setup without other specialized equipment and should be particularly useful for the study of cells that have low R_m or undergo rapid changes in R_a or R_m.

INTRODUCTION

Dynamic changes in passive cellular characteristics (access resistance, R_a, membrane resistance, R_m, and membrane capacitance, C_m) often occur during patch clamp recordings and may provide useful information regarding the state of the cell. In particular, rapid measurement of changes in C_m has been a useful indicator of membrane fusion or internalization events associated with exocytosis and endocytosis (Augustine and Neher, 1992; Breckenridge and Almers, 1987; Fernandez et al., 1984; Fidler and Fernandez, 1989; Neher and Marty, 1982; Neher, 1988; Zimmerberg et al., 1987). Several strategies have been developed to measure small changes in cellular capacitance: 1) adjustment of the capacitance compensation circuitry of the patch clamp amplifier (Hamill et al., 1981); 2) examination of the time constant associated with a step change in cellular potential (Lindau and Neher, 1988); 3) calculation of capacitance from a power spectral analysis of the input impedance using a pseudo-random binary sequence voltage perturbation (Joshi and Fernandez, 1988); and 4) measurement of current changes at a particular phase angle during sinusoidal perturbation of the cell's voltage (phase detection technique) (Breckenridge and Almers, 1987; Fernandez et al., 1984; Fidler and Fernandez, 1989; Lindau and Neher, 1988).

The phase detection technique that has been used in several laboratories offers the best temporal resolution of capacitance changes (Augustine and Neher, 1992; Fidler and Fernandez, 1989; Penner and Neher, 1989). Two variations of the phase detection technique have been employed for calculating the capacitance: 1) The absolute magnitude and phase of the current signal is measured and C_m is calculated from the current data combined with a separate measurement of membrane potential and holding current (Pusch and Neher, 1988). 2) The phase angle of a signal caused by the addition of a series resistance is identified, and a signal directly related to capacitance changes is assumed to occur orthogonal to that for resistance changes (Fidler and Fernandez, 1989; Joshi and Fernandez, 1988). Both techniques work well under many recording conditions, but both have some technical difficulties, particularly for cells of low membrane resistance. In the first method, changes in resting membrane potential will cause an artificial change in the capacitance signal and, in the second, a low R_m will cause the resistance perturbation vector to not be orthogonal to that for capacitance. In addition, the capacitance vector needs to be continually assessed over time, because it changes after any change in R_a, R_m, or C_m.

For my own experiments, I desired to examine changes in cellular resistance and capacitance of carotid body glomus cells during stimulation. Not only do some of these cells have a low membrane resistance (~200 MΩ), but resting membrane potential may change during stimulation (Donnelly, 1993). This made implementation of either standard phase detection technique problematic. Furthermore, I wanted an on-line assessment of absolute measures of R_a, R_m, and C_m without back-calculating the values after adjustment of the amplifier's compensation circuit, as required in the phase tracking technique (Fidler and Fernandez, 1989).

The following describes the development of an impedance measurement device for on-line assessment of R_a, R_m, and C_m with sufficient accuracy to indicate fusion events. The forcing functions and detection scheme are all implemented in software, and, thus, no specialized equipment is needed other than a conventional patch clamp recording setup. The model of a cell under patch clamp conditions and derivation

Received for publication 24 June 1993 and in final form 16 December 1993.
Address reprint requests to Dr. D. F. Donnelly, Department of Pediatrics, Division of Respiratory Medicine, Yale University School of Medicine, 333 Cedar St., New Haven, CT 06510.
© 1994 by the Biophysical Society
0006-3495/94/03/873/05 $2.00

of the equations follows closely that of Pusch and Neher (1988). Usefulness of the circuit was tested using rat peritoneal mast cells.

MATERIALS AND METHODS

Mast cell preparation and recording system

After anesthetization with penthrane, rat peritoneal mast cells were harvested by lavage with oxygenated Ringer's saline (in mM: 120 NaCl, 3 KCl, 1 $CaCl_2$, 1 $MgCl_2$, 24 HCO_3 equilibrated with 95% O_2, 5% CO_2). The cells were plated on glass cover slips covered with an adhesion chemical (Celltak, Collaborative Science, Cambridge, MA). During patch clamp recording, the external solution was HEPES buffered saline (in mM: 140 NaCl, 3 KCl, 1 $MgCl_2$, 1 $CaCl_2$, 10 HEPES, buffered to pH 7.4 at 26°C). The pipette solution was, in mM: 140 potassium glutamate, 10 HEPES, 7 $MgCl_2$, 3 KCl, 0.2 ATP, and 5 EGTA with the addition of 10 μM GTP-γS to stimulate degranulation (Fernandez et al., 1984; Fidler and Fernandez, 1989).

Pipette currents were recorded with an Axoclamp 1D patch clamp amplifier with 50 GΩ feedback resistance. The command potential was generated by an IBM AT-compatible computer (Gateway 486–50DX2, Sioux City, SD) and Tecmar Labmaster A/D interface (Scientific Solutions). Sine wave forcing functions were generated by approximating a sine wave function with 120 or 240 discrete points that were added together and sent to the digital-to-analog (D/A) converter (see Fig. 2). The delay between points was adjusted to produce frequencies of 333 and 666 Hz.

Calculation of cell parameters

The initial assumption was that a cell recorded under patch clamp may be modelled as an equivalent circuit with three unknowns (Fig. 1). The validity of this assumption was previously addressed (Joshi and Fernandez, 1988) and will not be considered here. The current through the current sensor, I_{sensor}, is the sum of the current through the cell and through the compensation circuit.

$$I_{sensor} = V_{sensor}Y_{cell} + (V_{sensor} - V_{comp})Y_{comp} \quad (1)$$

Since V_{comp} is $2V_{sensor}$ it follows that

$$Y_{cell} - Y_{comp} = I_{sensor}/V_{sensor} = Y_m \quad (2)$$

where Y_m is the measured conductance from the current sensor, Y_{comp} is the conductance of the compensation circuit, and Y_{cell} is the conductance of the cell/pipette combination. Thus, the conductance of the cell is the addition of the measured conductance and the conductance of the compensation circuitry, which may be directly read from the amplifier. The cell conductance may be solved as follows. Using the notation and development of Pusch and Neher (1988), the conductance of the pipette/cell combination ($Y_{cell}(\omega)$), in the Laplace plane, is determined by R_a and the parallel combination of C_m and R_m.

$$Y_{cell}(\omega) = A + iB = (1 + i\omega C_m R_m)/(R_a + R_m + iwC_m R_a R_m) \quad (3)$$

where $A = \mathrm{Re}(Y_{cell})$, $B = \mathrm{Im}(Y_{cell})$. Letting $b = 1/(R_a + R_m)$, $x = \omega C_m R_m$ and $a = R_a b$ and substituting gives

$$A = (b + abx^2)/(1 + a^2x^2) \quad (4)$$

$$B = (bx - abx)/(1 + a^2x^2) \quad (5)$$

Solving Eq. 4 for x^2, multiplying by a^2, and adding 1 yields

$$1 + a^2x^2 = (ba - b)/(Aa - b) \quad (6)$$

Inserting this into Eq. 5 yields

$$B = x(b - Aa) \quad (7)$$

Substituting and solving Eq. 7 at two frequencies, ω_1 and ω_2, where $\omega_2 = 2\omega_1$ gives

$$B_1 = x_1 b - A_1 a x_1 \quad (8)$$

$$B_2 = x_2 b - A_2 a x_2 = 2x_1 b - 2A_2 a x_1 \quad (9)$$

Solving Eqs. 8 and 9 for ax_1 gives

$$ax_1 = (B_2 - 2B_1)/(2A_1 - 2A_2) \quad (10)$$

and solving Eqs. 8 and 9 for bx_1 gives

$$bx_1 = B_1 + A_1 a x_1 \quad (11)$$

Access resistance, R_a, may be calculated from

$$R_a = ax_1/bx_1 \quad (12)$$

$$b = (A_1^2 R_a + B_1^2 R_a - A_1)/(R_a A_1 - 1) \quad (13)$$

Knowing b and R_a, R_m and C_m may be calculated

$$R_m = 1/b - R_a \quad (14)$$

$$C_m = (A_1 - b)/(\omega_1 R_a R_m B_1 b) \quad (15)$$

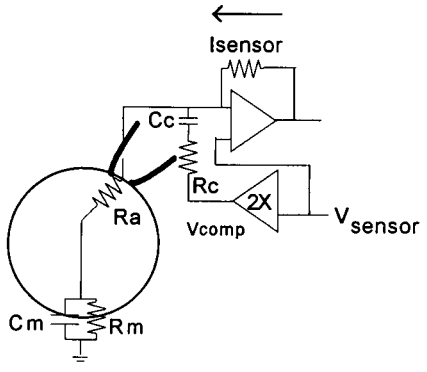

FIGURE 1 Equivalent circuit diagram of a patch-clamped cell. The cell under study is characterized by a passive membrane resistance (R_m) and membrane capacitance (C_m) and is recorded through a patch pipette having an access resistance (R_a). Current to the patch electrode may be delivered through the current sensor (I_{sensor}) or through the compensation circuit characterized by resistor, R_c, and capacitor C_c. The reference voltage is V_{sensor}.

Implementation

The sequence of implementation includes three steps.

Step 1: Estimation of the filter characteristics. To limit Johnson noise of the recording, low-pass filtering is generally used on the output of patch clamp amplifiers. This filter will reduce the amplitude and add a phase delay to the sine wave signals in the same way that changes in cell characteristics would alter the amplitude and phase. To compensate the filter effects, a signal of known phase and amplitude with respect to the driving signal is applied to the filter, and the output signal acquired. A filter compensation vector is thus calculated at each frequency, ω_1 and ω_2. These vectors may be used to correct the measured current signal sampled after the filter module to that present before the filter module.

Step 2: Estimate the conductance of the compensation circuit. It is generally desirable to record the electrode current at high gain to avoid noise resulting from digitization uncertainty (Bookman et al., 1991). To do so, most of the cell/pipette current must be delivered through the compensation circuit to avoid a rail condition. From Eq. 2, the cell conductance is the addition of the measured conductance and the conductance of the compensation circuit. The compensation circuit setting may be directly read from the amplifier and the conductance value calculated and directly added to the measured value: $Y_{comp} = C_c i\omega/(C_c R_c i\omega + 1)$.

Step 3: Once whole-cell recording conditions are established, the pipette voltage is driven with a combination of two harmonic frequencies superimposed on the holding potential. A/D samples are obtained at 8 points/cycle at the slower frequency or 4 points/cycle at the higher frequency and added or subtracted to obtain the current at each frequency (Fig. 2). Division of the current by the magnitude of the driving voltage gives the measured conductance, Y_m.

RESULTS

The effect of known changes in resistance or capacitance may be examined using a model cell, or, alternatively, by changing the compensation settings. This causes the output to change in the opposite direction, i.e., a compensation setting of 5 pF will appear on the output as a capacitance of −5 pF. In this case shown in Fig. 3, no electrode was connected to the head stage, and the net current through the current sensor came from the compensation circuit. With R_c set at 5, 10, or 50 MΩ, changes in calculated C_m closely followed the settings of the capacity compensation controls, C_c, over the range of 1–20 pF (Fig. 3). At high R_c, C_m was slightly underestimated (by 0.3 pF at 20 pF), and with a low R_c (5 MΩ), C_m was overestimated (by 0.2 pF), but the response lines were linear for a fixed value R_c. The source for the apparent error is uncertain and may be due to a slight misadjustment of the fast compensation control or due to a slight inaccuracy of the compensation control readout. Because these errors were within the uncertainties caused by stray capacitances, it was not possible to better resolve their origin.

The usefulness of the technique is demonstrated by observing degranulation of mast cells (Fig. 4). Degranulation was induced by the inclusion of GTPγS in the patch pipette fluid (Fernandez et al., 1984; Fidler and Fernandez, 1989).

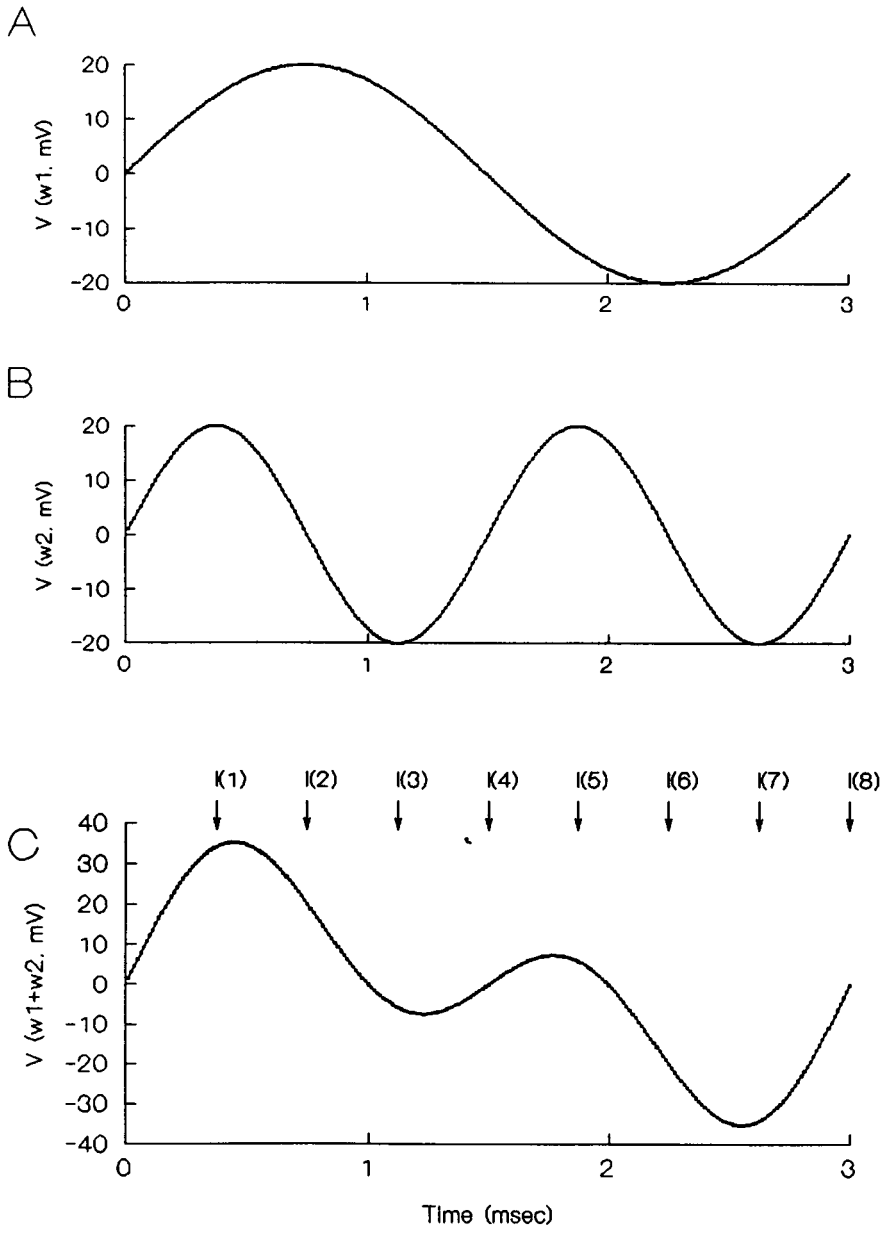

FIGURE 2 Implementation of the two-sine-wave technique. (*A*) The low- frequency sine wave (ω_1, 333 Hz) is generated using 240 discrete D/A points and is 20 mV p-p. (*B*) The high-frequency wave (ω_2, 666 Hz) is generated at 240 points/2 cycles and is also 20 mV p-p. (*C*) The forcing function applied to the cell/pipette is a linear summation of *A* and *B*. The output current is sampled eight times per cycle. $I(\omega_1) = 0.5\ \{I(2) - I(6) + i[I(4) - I(8)]\}$ $I(\omega_2) = 0.25\ \{I(1) - I(3) + I(5) - I(7) + i[I(2) - I(4) + I(6) - I(8)]\}$.

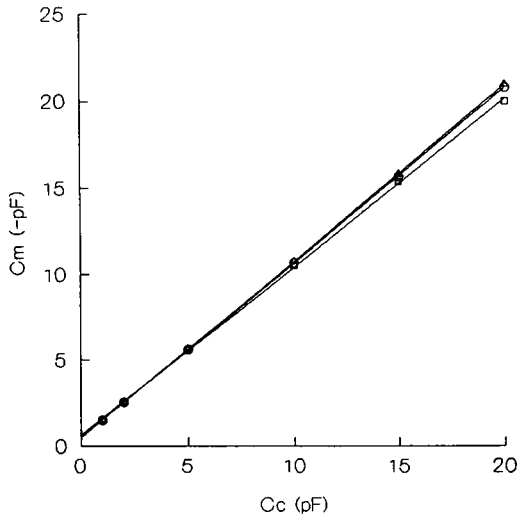

FIGURE 3 Change in calculated value of C_m following changes in the amplifier capacity compensation controls (C_c, R_c). No electrode was connected to the head stage; thus, the sensor current is equal to the current from the capacity compensation control. The compensation setting for R_c on the amplifier was fixed at 5 MΩ (○), 10 MΩ (△), or 50 MΩ (□).

Passive cellular parameters R_m, R_a, and C_m were calculated and displayed in real time. The values at low gain are shown in Fig. 4 and an excerpt at high gain is pictured as an inset to Fig. 4. For this experiment, the amplifier gain was set at 10 mV/pA and was a compromise between a high gain, which would better indicate individual fusion events, and a low gain, which allows for larger dynamic changes in R_m, R_a, and C_m. The cell shown in Fig. 4 was chosen because it displayed large dynamic swings in R_m, but this had no effect on the calculated values for R_a or C_m.

DISCUSSION

One of the most useful features of patch clamp recording has been for the study of exocytosis from secretory cells (Hamill et al., 1981; Neher and Marty, 1982; Neher, 1988). Fusion of the secretory vesicle with the external cell membrane results in a slight increase in cellular capacitance. Capacitance was initially monitored by readjustment of the compensation circuit of the patch clamp amplifier (Hamill et al., 1981), but for better time resolution, circuits were developed for con-

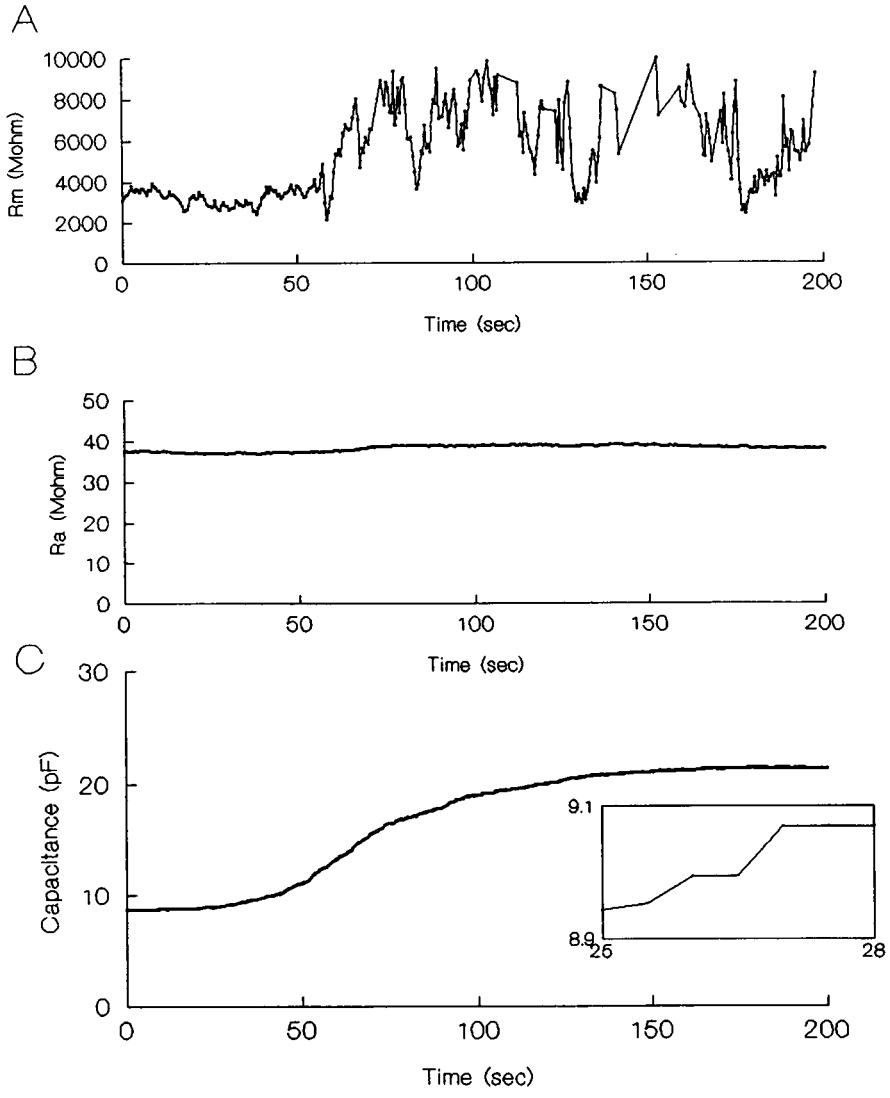

FIGURE 4 Calculation of time-dependent changes in R_a, R_m, and C_m during degranulation of a rat peritoneal mast cell. (*A*) Calculated values for R_m as a function of time. (*B*) Calculated values for R_a as a function of time. (*C*) Calculated values for C_m as a function of time during degranulation. *Inset:* Expanded tracing of capacitance changes over seconds 25–28. Note step-like changes in capacitance. Values were computed at stored at 2/s. This tracing was selected for the rather large spontaneous changes in R_m. Note independence of the changes in R_m and other traces.

tinuous assessment. As mentioned in the Introduction, the phase detection technique offers the best resolution and is generally implemented in one of two forms. In one form, the cell/pipette current is measured with no phase or amplitude distortion (i.e., no low-pass filter distortion) and, combined with measurements of resting potential and holding current, is used to calculate capacitance (Pusch and Neher, 1988). The second implementation is independent of filter distortion but relies on the accurate setting of a phase-sensitive detector such that the output is only changed by a change in cell capacitance (Joshi and Fernandez, 1988). This angle setting must be periodically ascertained because it changes with any change in R_a, R_m, or C_m, and a misadjustment of the phase angle setting of the detector will cause changes in R_a or R_m to appear on the capacitance trace.

The device described in this paper may offer a significant advantage over either technique given a set of recording conditions. In the first technique, a change in membrane potential across the physiological range may cause an apparent change in capacitance, especially in cells with a low R_m. Since resting potential is determined separately from the capacitance measurement, this may be easily missed. The second technique, or phase tracking technique (Fidler and Fernandez, 1989), may suffer three constraints. 1) If the phase angle changes significantly between phase resetting points, then interpretation of the data between these points is problematic. 2) If R_m is low, then the correct phase angle for detecting changes in C_m will not be the same as the angle for which the output is independent of changes in R_a. That is, the phase angle cannot be accurately set solely by dithering a series resistance. 3) The amplifier's compensation circuitry must be perfectly adjusted to provide a calibration signal to translate the output values into units of capacitance (Fidler and Fernandez, 1989). The present device offers independence of both of these concerns, since the calculation is not dependent on measurement of resting potential or identification of any specific phase angle. It may be implemented primarily in software and thus does not require specialized equipment other than a (relatively) fast computer and A/D interface. In addition, it offers the potential to measure dynamic changes in capacitance at a time of rapidly changing conductance, such as may occur during a depolarization step.

A complete analysis of the signal/noise as a function of frequency and detection technique is beyond the immediate scope of this paper; however, the present device should respect the same constraints as that for single frequency capacitance assessment (Pusch and Neher, 1988). The capacitance resolution per sine wave cycle is relatively constant up to a corner frequency determined by access resistance and membrane capacitance ($fc = 1/R_aC_m$). As long as the driving frequencies are below this value then a resolution 10–20 fF per sine wave cycle may be expected. Further noise reduction may be affected by low-pass filtering the output or averaging more sine wave cycles on the input.

In summary, the presently described technique offers a method of calculating passive cellular parameters during patch clamp recording. It offers the advantage of ease of use and is not dependent on specialized hardware beyond a common computer, A/D converter, and patch clamp amplifier. It also does not require an accurate adjustment of the compensation controls for translation of the calculated values into conventional units (pF and MΩ). This technique should be a useful alternative to the phase detection technique for the study of secreting cells, particular in cases where R_m is low or resting potential is changing.

REFERENCES

Augustine, G. J., and E. Neher. 1992. Calcium requirements for secretion in bovine chromaffin cells. *J. Physiol. (Lond.).* 450:247–271.

Bookman, R. J., N. Fidler-Lim, F. E. Schweizer, and M. Nowycky. 1991. Single cell assays of excitation-secretion coupling. *Ann. NY Acad. Sci.* 635:352–364.

Breckenridge, L. J., and W. Almers. 1987. Final steps in exocytosis observed in a cell with giant secretory granules. *Proc. Natl. Acad. Sci. USA.* 84: 1945–1949.

Donnelly, D. F. 1993. Response to cyanide of two types of glomoid cells in mature rat carotid body. *Brain Res.* 630:157–158.

Fernandez, J. M., E. Neher, and B. D. Gomperts. 1984. Capacitance measurements reveal stepwise fusion events in degranulating mast cells. *Nature.* 312:453–455.

Fidler, N., and J. M. Fernandez. 1989. Phase tracking: an improved phase detection technique for cell membrane capacitance measurements. *J. Biophys.* 56:1153–1162.

Hamill, O. P., A. Marty, E. Neher, B. Sakmann, and F. J. Sigworth. 1981. Improved patch-clamp techniques for high-resolution current recording from cells and cell-free membrane patches. *Pfluegers Arch.* 391:85–100.

Joshi, C., and J. M. Fernandez. 1988. Capacitance measurements: an analysis of the phase detector technique used to study exocytosis and endocytosis. *J. Biophys.* 53:885–892.

Lindau, M., and E. Neher. 1988. Patch-clamp techniques for time-resolved capacitance measurements in single cells. *Pfluegers Arch.* 411:137–146.

Neher, E. 1988. The influence of intracellular calcium concentration on degranulation of dialysed mast cells from rat peritoneum. *J. Physiol. (Lond.).* 395:193–214.

Neher, E., and A. Marty. 1982. Discrete changes of cell membrane capacitance observed under conditions of enhanced secretion in bovine adrenal chromaffin cells. *Proc. Natl. Acad. Sci. USA.* 79:6712–6716.

Penner, R., and E. Neher. 1989. The patch-clamp technique in the study of secretion. *Trends Neurosci.* 12:159–163.

Pusch, M., and E. Neher. 1988. Rates of diffusional exchange between small cells and a measuring patch pipette. *Pfluegers Arch.* 411:204–211.

Zimmerberg, J., M. Curran, F. S. Cohen, and M. Brodwick. 1987. Simultaneous electrical and optical measurements show that membrane fusion precedes secretory granule swelling during exocytosis of beige mouse mast cells. *Proc. Natl. Acad. Sci. USA.* 84:1585–1589.